

Nuclear transparencies in relativistic $A(e, e'p)$ models

P. Lava^a, M.C. Martínez^b, J. Ryckebusch^a, J.A. Caballero^b,
J.M. Udías^c

^a*Department of Subatomic and Radiation Physics, Ghent University,
Proeftuinstraat 86, B-9000 Gent, Belgium*

^b*Departamento de Física Atómica, Molecular y Nuclear, Universidad de Sevilla,
Apdo. 1065, E-41080 Sevilla, Spain*

^c*Departamento de Física Atómica, Molecular y Nuclear, Facultad de Ciencias
Físicas, Universidad Complutense de Madrid, E-28040 Madrid, Spain*

Abstract

Relativistic and unfactorized calculations for the nuclear transparency extracted from exclusive $A(e, e'p)$ reactions for $0.3 \leq Q^2 \leq 10$ (GeV/c)² are presented for the target nuclei C, Si, Fe and Pb. For $Q^2 \geq 0.6$ (GeV/c)², the transparency results are computed within the framework of the recently developed relativistic multiple-scattering Glauber approximation (RMSGa). The target-mass and Q^2 dependence of the RMSGa predictions are compared with relativistic distorted-wave impulse approximation (RDWIA) calculations. Despite the very different model assumptions underlying the treatment of the final-state interactions in the RMSGa and RDWIA frameworks, they predict comparable nuclear transparencies for kinematic regimes where both models are applicable.

Key words: Relativistic models, Optical potentials, Glauber theory, Nuclear transparency;

PACS: 24.10.Jv, 24.10.-i, 24.10.Ht, 25.30.Dh

The transparency of the nuclear medium to the propagation of protons is an issue of fundamental importance. The nuclear transparency provides a measure of the probability that a proton of a certain energy escapes from the nucleus without enduring inelastic final-state interactions (FSI). The nuclear transparency is a useful quantity for studying nuclear medium effects, and in particular, it is very well suited for investigations of the so-called color transparency (CT) phenomenon, which predicts a significant enhancement of

Email address: Jan.Ryckebusch@ugent.be (J. Ryckebusch).

the transmission of protons through nuclei [1,2] once QCD mechanisms start playing a role.

During the last decade, several investigations of the nuclear transparency have been carried out using the $A(e, e'p)$ reaction in the quasi-elastic (QE) regime. In this kinematic regime, the impulse approximation (IA), where a quasifree single-nucleon knockout reaction mechanism is assumed, has been proved to provide a good description of the reaction dynamics. Thanks to the electromagnetic character of the initial-state interactions in an $A(e, e'p)$ process, the entire nuclear volume can be probed.

Nuclear transparency measurements with the $A(e, e'p)$ reaction are available for a range of target nuclei. The first experiments were performed at Bates for $Q^2 \approx 0.3$ (GeV/c)² [3], and at SLAC for $1 \leq Q^2 \leq 7$ (GeV/c)² [4,5]. Recently, measurements at the Thomas Jefferson National Accelerator Facility (TJNAF) provided precise data for the target nuclei ²D, ¹²C and ⁵⁶Fe and $Q^2 = 3.3, 6.1$ and 8.1 (GeV/c)² [6]. The same facility provided an alternate set of data for the target nuclei ¹²C, ⁵⁶Fe and ¹⁹⁷Au and $0.64 \leq Q^2 \leq 3.25$ (GeV/c)² [7,8].

The prediction of the nuclear transparency to protons poses a serious challenge for models dealing with the $A(e, e'p)$ reaction due to the wide range of proton energies which are probed in the present-day experiments. As a matter of fact, at present there is no uniform and realistic framework in which the proton-nucleus FSI effects can be computed for proton kinetic energies ranging from 0.3 to several GeV. For kinetic energies up to around 1 GeV, most theoretical $A(e, e'p)$ investigations are performed within the context of the Distorted-Wave Impulse Approximation (DWIA), where the effect of the scatterings on the emerging nucleon is estimated with the aid of proton-nucleus optical potentials. The parameterizations of these potentials are usually not available for proton kinetic energies T_p beyond 1 GeV. Beyond this energy, the Glauber model, which is a multiple-scattering extension of the eikonal approximation, offers a valid and economical alternative for describing FSI. In a Glauber framework, the effects of FSI on the $A(e, e'p)$ observables are computed directly from the elementary proton-nucleon scattering data through the introduction of a profile function. The Glauber method postulates linear trajectories and frozen spectator nucleons, and the lower limit of this treatment to $A(e, e'p)$ has not yet been established.

Numerous predictions for the nuclear transparencies within the context of non-relativistic Glauber theory have been reported in literature [9,10,11,12,13,14,15,16,17]. These results are typically obtained in a non-relativistic and factorized model for dealing with the $e + A \rightarrow e' + (A - 1) + p$ reaction dynamics. In this context, non-relativistic refers to the fact that the calculations use bound-state wave functions or nuclear densities from solutions to a Schrödinger equation and non-relativistic expressions for the electromagnetic photon-nucleus inter-

action Lagrangian. In the context of modeling $A(e, e'p)$ processes, factorization refers to the approximation of decoupling the electron-proton from the nuclear dynamics part in the calculations.

In this paper we focus on relativistic and unfactorized descriptions of nuclear transparencies extracted from quasi-elastic $A(e, e'p)$ processes. In the past, relativistic distorted-wave impulse approximation (RDWIA) $A(e, e'p)$ calculations for the nuclear transparency have been presented by Kelly [18] and Meucci [19]. Kelly used an effective current operator containing the Dirac potentials, two-component bound states and distorted waves obtained as solutions to relativized Schrödinger equations. Meucci used bound-state wave functions from a relativistic mean-field approach, while the effective Pauli reduction was adopted to construct the ejectile's wave function.

For $T_p \geq 1$ GeV many partial waves need to be computed, thus a description of the FSI mechanisms in terms of phenomenological optical potentials may not be the most economical way at higher energies. In addition, the global optical potentials we use in this work were fitted to data with a limited range in T_p below 1 GeV, hence the RDWIA studies of the nuclear transparency do not cover the kinematic ranges beyond $T_p=1$ GeV.

Recently, a relativized and unfactorized version of the Glauber model has been proposed [20,21,22]. In this paper, transparencies obtained within this so-called relativistic multiple-scattering Glauber approximation (RMSGGA) framework will be compared with those obtained in the RDWIA framework as it has been implemented by the Madrid-Sevilla group [23,24,25,26]. The comparison is made in a consistent way. For the transparency results which will be presented below, this implies that the two frameworks only differ in the way they treat the final-state interactions. All the remaining ingredients are kept identical.

In what follows we will first sketch the basic ingredients entering the RDWIA and the RMSGGA frameworks, thereby indicating the similarities and differences between the two. Then, the energy dependence, expressed in terms of the four-momentum transfer $Q^2 = q^2 - \omega^2$, and target-mass dependence of the nuclear transparencies obtained in the two approaches will be compared and confronted with the data.

Adopting the IA, the central quantity to be computed in a relativistic approach to $A(e, e'p)$ is the current matrix element

$$\langle J^\mu \rangle = \int d\vec{r} \bar{\phi}_F(\vec{r}) \hat{J}^\mu(\vec{r}) e^{i\vec{q}\cdot\vec{r}} \phi_B(\vec{r}), \quad (1)$$

where ϕ_B and ϕ_F are relativistic wave functions describing the initial bound and final outgoing nucleon respectively. Further, \hat{J}^μ is the relativistic one-body

current operator. The bound-state wave function ϕ_B is a four-spinor with well-defined parity and angular momentum quantum numbers (κ_b, μ_b) , obtained within the framework of the relativistic independent-particle shell model. It may be formally written as

$$\phi_B(\vec{r}) = \begin{pmatrix} g_{\kappa_b}(r)\Phi_{\kappa_b}^{\mu_b}(\Omega_r) \\ if_{\kappa_b}(r)\Phi_{-\kappa_b}^{\mu_b}(\Omega_r) \end{pmatrix}, \quad (2)$$

with $\Phi_{\kappa_b}^{\mu_b}(\Omega_r)$ the usual spin spherical harmonics. The quantum numbers of the bound-state ϕ_B reflect the nature of the single-hole state in which the residual nucleus is left.

Within the RDWIA framework, ϕ_F is a scattering solution to a Dirac-like equation, which includes scalar (S) and vector (V) global optical potentials obtained by fitting elastic *proton – nucleus* scattering data. The scattering wave function, expressed in terms of a partial-wave expansion in configuration space, reads

$$\phi_F(\vec{r}) = 4\pi\sqrt{\frac{E_F + M}{2E_F}} \sum_{\kappa\mu m} e^{-i\delta_{\kappa}^*} i^{\ell} \langle \ell m \frac{1}{2} s_F | j \mu \rangle Y_{\ell}^{m*}(\Omega_{p_F}) \Psi_{\kappa}^{\mu}(\vec{r}), \quad (3)$$

where $\Psi_{\kappa}^{\mu}(\vec{r})$ are four-spinors of the same form as in Eq. (2), except for the fact that they have complex phase-shifts and radial functions. The outgoing nucleon momentum, energy and spin are denoted as \vec{p}_F , E_F and s_F respectively.

In the RMSGA framework, the scattering wave function takes on the following form

$$\phi_F(\vec{r}) \equiv \phi_{p_F s_F}(\vec{r})\mathcal{G}(\vec{b}, z), \quad (4)$$

where $\phi_{p_F s_F}$ is a relativistic plane wave. The entire effect of the FSI mechanisms is contained in the Dirac-Glauber phase $\mathcal{G}(\vec{b}, z)$, which is an A-body operator and reads

$$\mathcal{G}(\vec{b}, z) = \prod_{\alpha \neq B} \left[1 - \int d\vec{r}' |\phi_{\alpha}(\vec{r}')|^2 \theta(z' - z) \Gamma(\vec{b} - \vec{b}') \right], \quad (5)$$

where the profile function for pN scattering is defined as

$$\Gamma(\vec{b}) = \frac{\sigma_{pN}^{tot}(1 - i\epsilon_{pN})}{4\pi\beta_{pN}^2} \exp\left(\frac{-b^2}{2\beta_{pN}^2}\right). \quad (6)$$

The parameters σ_{pN}^{tot} , β_{pN} and ϵ_{pN} depend on the proton kinetic energy and are obtained through interpolation of the data base available from the Particle Data Group [27]. We wish to stress that Glauber-based models come in very different flavours and that the RMSGA formulation used here borrows a lot of ingredients from the RDWIA approach to $A(e, e'p)$ processes, except for the way of computing the effect of FSI mechanisms on the hit proton, which is through-and-through different.

In order to make the comparisons between the RDWIA and RMSGA transparency predictions as meaningful as possible, all the ingredients in the $A(e, e'p)$ calculations not related to FSI, as those concerning the implementation of relativistic dynamics and nuclear recoil effects, are kept identical. In particular, both pictures use the relativistic bound-state wave functions from a Hartree calculation with the W1 parameterization for the different field strengths [28]. Further, all the results presented in this work are obtained within the Coulomb gauge using the so-called *CC2* current operator [29]. For the description of nuclear transparencies, the effect of Coulomb distortions has been recognized as negligible [18]. Therefore, no attempt has been made to correct for the Coulomb-distortion effect.

We wish to stress that the RDWIA, as implemented by the Madrid-Sevilla group, and RMSGA codes adopt very different numerical techniques to compute the scattering wave functions and the corresponding matrix elements of Eq. (1). The Madrid RDWIA code employs a partial-wave expansion to solve the Dirac equation for the ejectile. The cylindrical symmetry of the Glauber phase of Eq. (5) prohibits any meaningful use of this technique in the RMSGA calculations. Instead, the multi-dimensional integrals are computed numerically. In the limit of vanishing FSI mechanisms, however, the two codes should predict identical results. In the Glauber approach this limit is reached by putting the Glauber phase of Eq. (5) equal to unity. In the RDWIA picture, the effect of FSI can be made vanishing by nullifying the optical potentials when solving the differential equations for the radial wave functions determining the outgoing nucleon wave functions. In this so-called relativistic plane-wave impulse approximation (RPWIA) limit, the Madrid code is practically exact, as has been checked by comparing the partial-wave expansion results with the analytical ones [30]. In this plane-wave limit and assuming identical input options, the RMSGA-Gent and RDWIA-Madrid codes produce differential cross sections with an agreement to better than 5%. This discrepancy can be partially attributed to the numerical evaluation of the multi-dimensional integrals in RMSGA. This comparison gives us confidence about the consistency of the calculations.

The nuclear transparency provides a measure of the likelihood that a struck nucleon with kinetic energy T_p escapes from the nucleus. The nuclear transparency can be extracted from the measured $A(e, e'p)$ differential cross sections

$d^5\sigma^{exp}(e, e'p)$ on the basis of the following ratio

$$T_{exp}(Q^2) = \frac{\int_{\Delta^3 p_m} d\vec{p}_m \int_{\Delta E_m} dE_m S_{exp}(\vec{p}_m, E_m, \vec{p}_F)}{c_A \int_{\Delta^3 p_m} d\vec{p}_m \int_{\Delta E_m} dE_m S_{PWIA}(\vec{p}_m, E_m)}. \quad (7)$$

Here, S_{exp} is the experimentally determined reduced cross section

$$S_{exp}(\vec{p}_m, E_m, \vec{p}_F) = \frac{\frac{d^5\sigma^{exp}}{d\Omega_p d\epsilon' d\Omega_{e'}}(e, e'p)}{K\sigma_{ep}}, \quad (8)$$

where K is a kinematical factor and σ_{ep} is the off-shell electron-proton cross section, which is usually evaluated with the $CC1$ prescription of de Forest [29]. The quantities $\Delta^3 p_m$ and ΔE_m specify the phase-space volume in the missing momentum and energy and are commonly defined by the cuts $|p_m| \leq 300$ MeV/c and $E_m \leq 80$ MeV. These kinematic cuts, in combination with the requirement that the Bjorken variable $x = \frac{Q^2}{2M_p\omega} \approx 1$, guarantee that the electro-induced proton-emission process is predominantly quasi-elastic. For example, the effects of two-body meson-exchange and isobar currents, which are neglected within the IA, have been shown to be at the percent level for quasi-elastic kinematics [31,32].

In the above equation, S_{PWIA} is the reduced cross section within the plane-wave impulse approximation (PWIA) in the non-relativistic limit. The factor c_A in the denominator of Eq. (7) has been introduced to correct in a phenomenological way for short-range mechanisms and is assumed to be moderately target-mass dependent. It accounts for the fact that short-range correlations move a fraction of the single-particle strength to higher missing energies and momenta and, hence, beyond the ranges covered in the integrations $\int d\vec{p}_m \int dE_m$ of Eq. (7). The values for c_A which are adopted to extract the transparency from the $A(e, e'p)$ measurements are 0.9 (^{12}C), 0.88 (^{28}Si), 0.82 (^{56}Fe) and 0.77 (^{208}Pb).

Theoretically, the nuclear transparencies are extracted from the computed relativistic $A(e, e'p)$ angular cross sections for the individual single-particle states, according to

$$T_{theo}(Q^2) = \frac{\sum_{\alpha} \int_{\Delta^3 p_m} d\vec{p}_m S^{\alpha}(\vec{p}_m, E_m, \vec{p}_F)}{c_A \sum_{\alpha} \int_{\Delta^3 p_m} d\vec{p}_m S_{PWIA}^{\alpha}(\vec{p}_m, E_m)}. \quad (9)$$

This expression reflects the one used to determine T_{exp} . Indeed, in our approach, we obtain the ‘‘theoretical’’ transparencies by adopting identical expressions and cuts as in the experiments. Essentially, we replace the measured $A(e, e'p)$ angular cross sections by the computed ones. In addition, the integration over the missing energy $\int_{\Delta E_m} dE_m$ has been substituted by a sum over all

occupied shells (Σ_α) in the ground state of the target nucleus. Indeed, the relativistic Hartree approximation does predict bound-state eigenfunctions with a fixed energy-eigenvalue and zero width. When determining the denominator in Eq. (9), in our calculations the PWIA limit is accomplished by nullifying all sources of FSI mechanisms and neglecting those contributions introduced by the presence of negative-energy components in the relativistic bound nucleon wave function [30].

Transparencies have been calculated for the nuclei ^{12}C , ^{28}Si , ^{56}Fe and ^{208}Pb . All numerical calculations are performed in planar and constant (q, ω) kinematics. The adopted values for q and ω are the central values of the kinematics in the $A(e, e'p)$ transparency experiments reported in Refs. [3,4,7,8]. For each shell α , the kinetic energy of the outgoing nucleon is calculated by means of the relationship $T_p = \omega + \epsilon_\alpha$, where ϵ_α is the energy eigenvalue of the corresponding single-particle state. Due to the internal motion of the confined protons, the ejected protons emerge in a cone about the transferred momentum. The boundaries of the cone are restricted by the requirement that the “initial ” proton momentum $|p_m| \leq 300 \text{ MeV}/c$.

In the RDWIA calculations, we have employed the global $S - V$ parameterizations of Cooper et al [33], which provide the best phenomenological optical potentials to date. As the highest kinetic energy in these parametrizations is 1 GeV, RDWIA transparencies are obtained up to four-momentum transfers of $Q^2 \approx 1.8 (\text{GeV}/c)^2$. Due to its use of the eikonal approximation, the validity of RMSGA becomes questionable when approaching low values of Q^2 . For this reason the RMSGA model is not used for calculating transparencies below $Q^2 \approx 0.6 (\text{GeV}/c)^2$. Hence, the kinematic range $0.6 \leq Q^2 \leq 1.8 (\text{GeV}/c)^2$ will be covered in both the RMSGA and the RDWIA frameworks.

First, we investigate the sensitivity of the computed transparencies to the adopted parameterizations for the optical potentials. In Fig. 1 results for ^{12}C and ^{208}Pb are displayed as a function of Q^2 for different optical-potential parameterizations contained in Ref. [33]. For ^{12}C , both the predicted Q^2 dependence and the value of the transparency depend on whether A-dependent (EDAD1/EDAD2) or A-independent (EDAIC) fits for the potentials are selected. For ^{208}Pb , the noted differences between the different types of optical-potential sets are less pronounced. Within the class of A-dependent parameterizations, the versions EDAD1 and EDAD2 give rise to comparable nuclear transparencies. In the remainder of the paper, the EDAD1 version will be used. There are various arguments to motivate this choice. First, the A-independent parameterization is only available for a very limited number of nuclei, and extrapolation to other nuclei has been discouraged [33]. Second, all energy-dependent A-dependent parameterizations in Ref. [33] produce similar transparency predictions. Finally, the relativistic transparency calculations by Kelly [18] and Meucci [19] employed the EDAD1 parametrization. Adopting

the same choice makes easier the comparison between these predictions and ours.

In Fig. 2, the transparencies predicted by the RMSGGA and RDWIA models are displayed as a function of Q^2 and compared to the world data. The ^{197}Au data are compared to ^{208}Pb calculations. The RDWIA approach systematically underestimates the data by roughly 5 – 10%. The presented RDWIA transparency results for ^{56}Fe and ^{208}Pb are in better agreement with the data than those reported in [7]. The RDWIA transparencies obtained in Ref. [19], on the other hand, are rather comparable to ours for low Q^2 , the differences increasing for higher values.

The RMSGGA framework reproduces the ^{12}C data. With increasing target mass, the agreement worsens, mostly for the lower values of Q^2 . The quality of agreement achieved for ^{12}C and the systematic underprediction of the transparencies for heavier nuclei, was also a feature of the non-relativistic and factorized Glauber calculations of Pandharipande and Pieper [6,16]. A global feature of the RDWIA and RMSGGA calculations presented here, is that they tend to underestimate the measured transparencies. Note that this is at variance with the RDWIA calculations of [19].

As can be inferred from Fig. 2, the RMSGGA framework predicts less absorption than RDWIA for a light nucleus like ^{12}C . With increasing target mass the opposite holds true and when approaching the heaviest target nuclei considered here, the Glauber framework predicts 5 to 10 percent more absorption. The measured Q^2 dependence is reasonably well reproduced by both relativistic calculations. For low Q^2 the models reproduce the trend of decreasing transparencies. For $Q^2 \geq 2 \text{ (GeV/c)}^2$, the RMSGGA transparencies are close to constant, in line with the measured ones and those predicted in typical non-relativistic Glauber models. In fact, the modest energy variation of the transparency in the RMSGGA model is a reflection of the fact that the total and elastic proton-nucleon cross sections remain fairly constant once $T_p \geq 1.7 \text{ GeV}$.

In Ref. [18] large discrepancies were observed between the DWIA $A(e, e'p)$ transparencies and the ones from Glauber calculations of Nikolaev [10,11]. In contradistinction, Fig. 2 indicates reasonably good agreement between our RDWIA and RMSGGA model predictions for the medium-heavy nucleus ^{56}Fe and modest variations in opposite directions when moving to a lighter or heavier nucleus. In Ref. [18] the noted differences between the transparencies obtained from DWIA and those from the particular Glauber approach of Refs. [10,11], are attributed to the fact that the latter adopts a closure property in deriving the expression for the attenuation factor. We wish to stress that this approximation is NOT used in the RMSGGA formulation of Glauber theory. In computing the effect of FSI mechanisms on the the $A(e, e'p)$ cross sections, the sum extending over the occupied states α in Eq. (9) is carried

out in a similar fashion in RMSGA and RDWIA.

Investigating the attenuation for each individual shell in the target nucleus allows one to study the radial dependence of the FSI mechanisms. In the ^{12}C case, for example, the $1s_{1/2}$ has spatial characteristics which are very different from the $1p_{3/2}$ orbit. The attenuation for the individual states represents also a more stringent test of the (non-)similarity of the optical-potential and Glauber-based models for describing proton propagation through nuclei. In Fig. 3, the RMSGA and RDWIA predictions for the attenuation for the individual shells in ^{12}C are compared. These numbers are computed according to the definition of Eq. (9) without performing the sum over the states α . Obviously, the optical-potential approach predicts more absorption for both shells. As expected, both models predict a stronger attenuation for proton emission from a level which has a larger fraction of its density in the nuclear interior. Again, the results of Fig. 3 illustrate that the proton-nucleus (RDWIA) picture and the proton-nucleon picture (RMSGA) are not dramatically different in their predictions. These findings provide us additional confidence that the “low-energy” and “high-energy” regime can be bridged in a relatively smooth manner. Note further that the observed tendency of increasing ^{12}C transparencies at low Q^2 , can almost be entirely attributed to the $1s_{1/2}$ orbital.

The A-dependence of the nuclear transparencies at various values of the four-momentum transfer is studied in Fig. 4. The RDWIA framework reproduces the measured A-dependence, while RMSGA slightly overestimates it. Under the assumption that the attenuation effect is proportional to the radius of the target nucleus one would naively expect that the A-dependence of the nuclear transparency can be parameterized as

$$T(Q^2)=c(Q^2)A^{-\alpha(Q^2)} , \quad (10)$$

with $\alpha=1/3$. In the work of Ref. [7] it was shown that the dependence of $T_{exp}(Q^2)$ on the mass number could be nicely fitted with $c(Q^2) \equiv 1$ and $\alpha \equiv 0.17 \pm 0.04(Q^2=0.65)$, $0.22 \pm 0.05(Q^2=1.3)$, $0.24 \pm 0.04(Q^2=1.8)$, $0.25 \pm 0.04(Q^2=3.3)$, $0.20 \pm 0.02(Q^2=6.8)$. To guide the eyes these curves are also displayed in Fig. 4.

In conclusion, we have presented for the first time a relativistic calculation for the nuclear transparency for the process $e + A \rightarrow e' + (A - 1) + p$ covering the wide range of quasi-elastic kinematics in which experiments have been performed. An optical-potential approach has been used up to the highest kinetic energy ($T_p \approx 1$ GeV) for which potentials are readily available. Beyond that region we gathered our results within the context of a relativized and unfactorized Glauber framework. In a medium- Q^2 range, both models have been applied and their predictions compared. Both frameworks accommodate

relativistic effects in the bound-state and scattering wave functions, as well as in the electromagnetic current operator. Despite the very different assumptions underlying the description of FSI effects in an optical-potential and Glauber based approach to $A(e, e'p)$, their predictions for the nuclear transparency and, in general, the effect of attenuation for different single-particle levels, are comparable.

This work was partially supported by DGI (Spain) under Contracts Nos BFM2002-03315, FPA2002-04181-C04-04, BFM2000-0600 and BFM2003-04147-C02-01, by the Junta de Andalucía and by FWO-Flanders (Belgium) under Contract No G.0020.03. M.C.M. acknowledges financial support from the Fundación Cámara (University of Sevilla).

References

- [1] A. H. Mueller, in: Proc. XVII Rencontre de Moriond (Les Arcs, France), ed. Tran Thanh Van (Editions Frontieres, Gif-sur-Yvette, 1982) p. 13.
- [2] S. J. Brodsky, in: Proc. XIII Int. Symp. on multiparticle dynamics (Volendam, The Netherlands), eds. E.W. Kittel, W. Metzger, and A. Stergion (World Scientific, Singapore, 1982) p. 963.
- [3] G. Garino et al., Phys. Rev. C 45 (1992) 780.
- [4] T. O'Neill et al., Phys. Lett. B 351 (1995) 87.
- [5] N. Makins et al., Phys. Rev. Lett. 72 (1994) 1986.
- [6] K. Garrow et al., Phys. Rev. C 66 (2002) 044613.
- [7] D. Abbott et al., Phys. Rev. Lett. 80 (1998) 5072.
- [8] D. Dutta, Phys. Rev. C 68 (2003) 064603.
- [9] S. Frankel, W. Frati, and N. Walet, Nucl. Phys. A 580 (1994) 595.
- [10] N. N. Nikolaev, A. Szcurek, J. Speth, J. Wambach, B. G. Zakharov, and V. R. Zoller, Phys. Rev. C 50 (1994) R1296.
- [11] N. N. Nikolaev, A. Szcurek, J. Speth, J. Wambach, B. G. Zakharov, and V. R. Zoller, Nucl. Phys. A 582 (1995) 665.
- [12] Y. Golubeva, L. Kondratyuk, A. Bianconi, S. Boffi, and M. Radici, Phys. Rev. C 57 (1998) 2618.
- [13] L. Frankfurt, M. Strikman, and M. Zhalov, Phys. Rev. C 50 (1994) 2189.
- [14] L. Frankfurt, E. Moniz, M. Sargsyan, and M. Strikman, Phys. Rev. C 51 (1995) 3435.

- [15] L. Frankfurt, M. Strikman, and M. Zhalov, Phys. Lett. B 503 (2001) 73.
- [16] V. Pandharipande, S. Pieper, Phys. Rev. C 45 (1992) 791.
- [17] A. Kohama, K. Yazaki, and R. Seki, Nucl. Phys. A 551 (1993) 687.
- [18] J. J. Kelly, Phys. Rev. C 54 (1996) 2547.
- [19] A. Meucci, Phys. Rev. C 65 (2002) 044601.
- [20] D. Debruyne, and J. Ryckebusch, Nucl. Phys. A 699 (2002) 65.
- [21] D. Debruyne, J. Ryckebusch, S. Janssen, and T. Van Cauteren, Phys. Lett. B 527 (2002) 62.
- [22] J. Ryckebusch, D. Debruyne, P. Lava, S. Janssen, B. Van Overmeire, and T. Van Cauteren, Nucl. Phys. A 728 (2003) 226.
- [23] J. M. Udias, P. Sarriguren, E. Moya de Guerra, E. Garrido, J. A. Caballero, Phys. Rev. C 48 (1993) 2731.
- [24] J. M. Udias, P. Sarriguren, E. Moya de Guerra, E. Garrido, J. A. Caballero, Phys. Rev. C 51 (1995) 3246.
- [25] J. M. Udias, J. A. Caballero, E. Moya de Guerra, J. E. Amaro, T. W. Donnelly, Phys. Rev. Lett. 83 (1999) 5451.
- [26] J. M. Udias, J. A. Caballero, E. Moya de Guerra, J. R. Vignote, A. Escuderos, Phys. Rev. C 64 (2001) 024614.
- [27] K. Hagiwara et al., Phys. Rev. D 66 (2002) 010001, <http://pdg.lbl.gov/>
- [28] Furnstahl et al., Nucl. Phys. A 615 (1997) 441.
- [29] T. de Forest, Nucl. Phys. A 392 (1983) 232.
- [30] J. A. Caballero, T. W. Donnelly, E. Moya de Guerra, J. M. Udias, Nucl. Phys. A 632 (1998) 323.
- [31] J. Ryckebusch, Phys. Rev. C 64 (2001) 044606.
- [32] J. E. Amaro, M. B. Barbaro, J. A. Caballero, F. Kazemi Tabatabaei, Phys. Rev. C 68 (2003) 014604.
- [33] E. D. Cooper, S. Hama, B. C. Clark, and R. L. Mercer, Phys. Rev. C 47 (1993) 297.

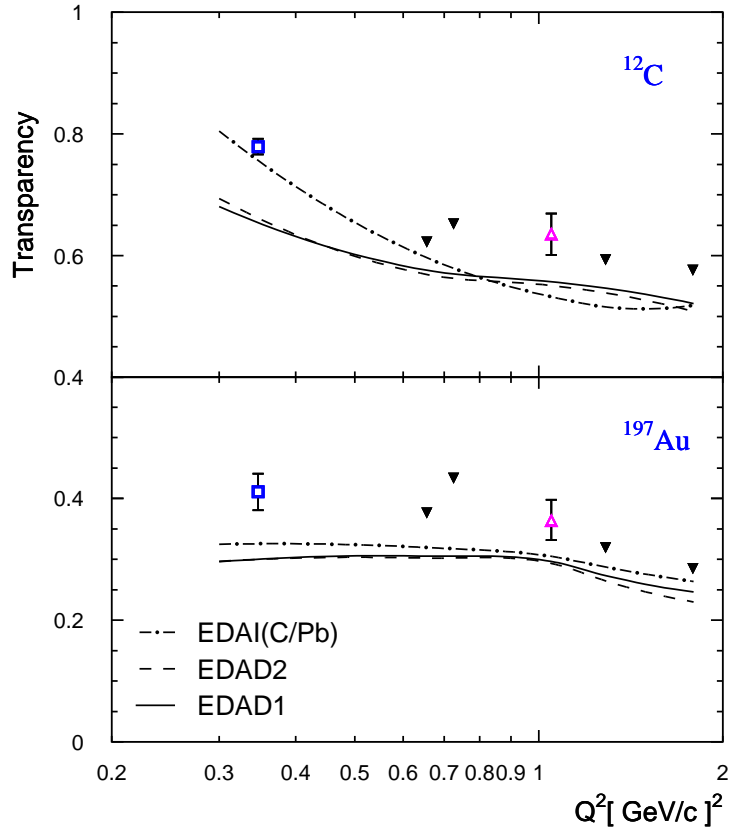


Fig. 1. The sensitivity of the computed nuclear transparencies in ¹²C and ¹⁹⁷Au to the adopted choice for the parameterization of the relativistic optical potentials. Results of RDWIA calculations with the EDAD1 (solid curve), EDAD2 (dashed curve) and EDAI(C/Pb) (dot-dashed curve) are shown. Data points are from Refs. [3] (open squares), [4,5] (open triangles), and [7,8](solid triangles)

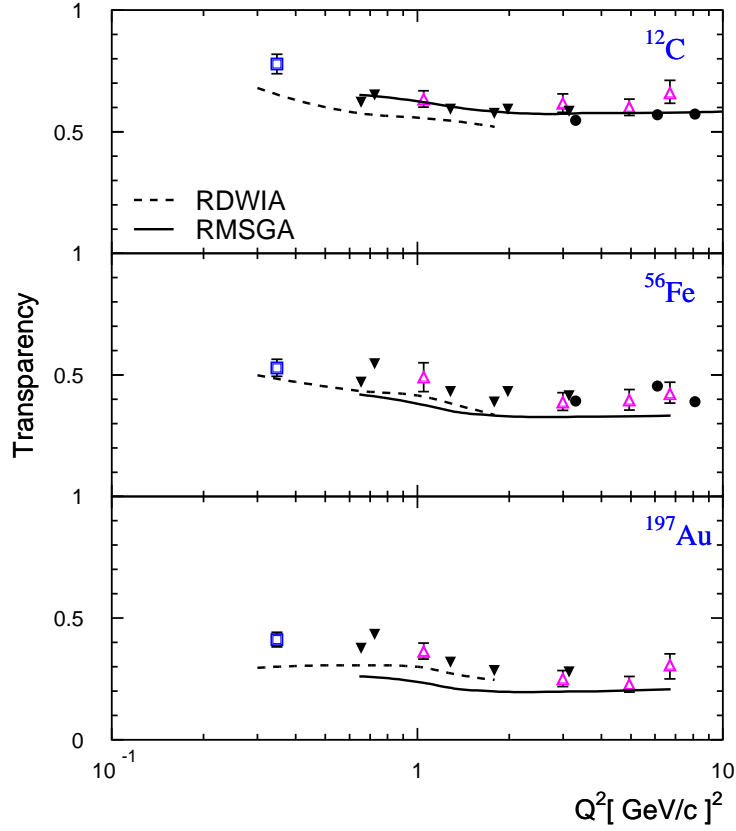


Fig. 2. Nuclear transparencies versus Q^2 for $A(e, e'p)$ reactions in quasi-elastic kinematics. The RMSGA (solid lines) are compared to the RDWIA (dashed lines) results. Data are from Refs. [3] (open squares), [4,5] (open triangles), [6](solid circles) and [7,8](solid triangles).

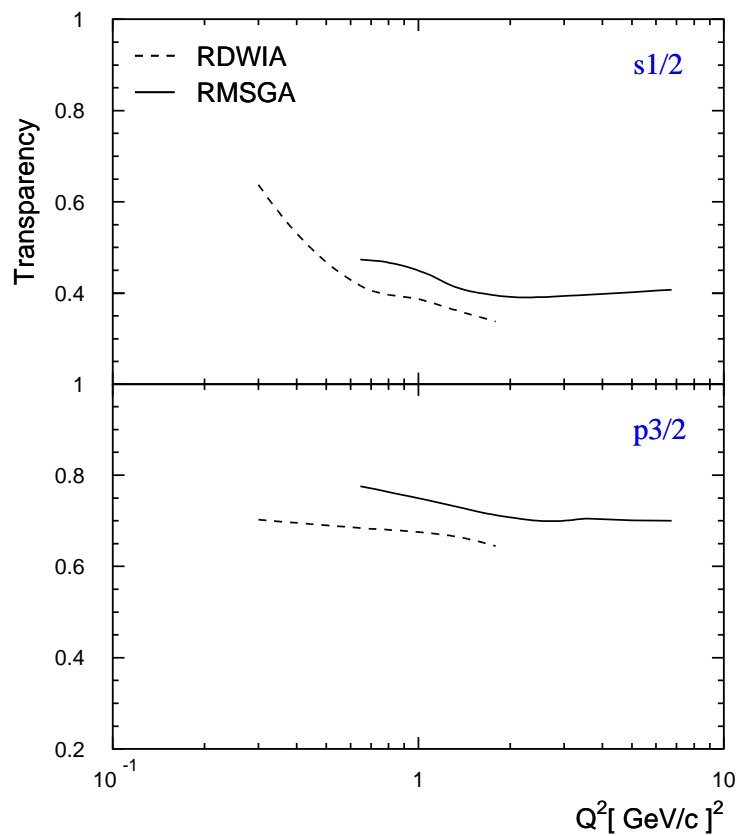


Fig. 3. The Q^2 dependence of the computed nuclear transparency for the two single-particle orbits in ^{12}C as obtained in the RDWIA and RMSGGA approach.

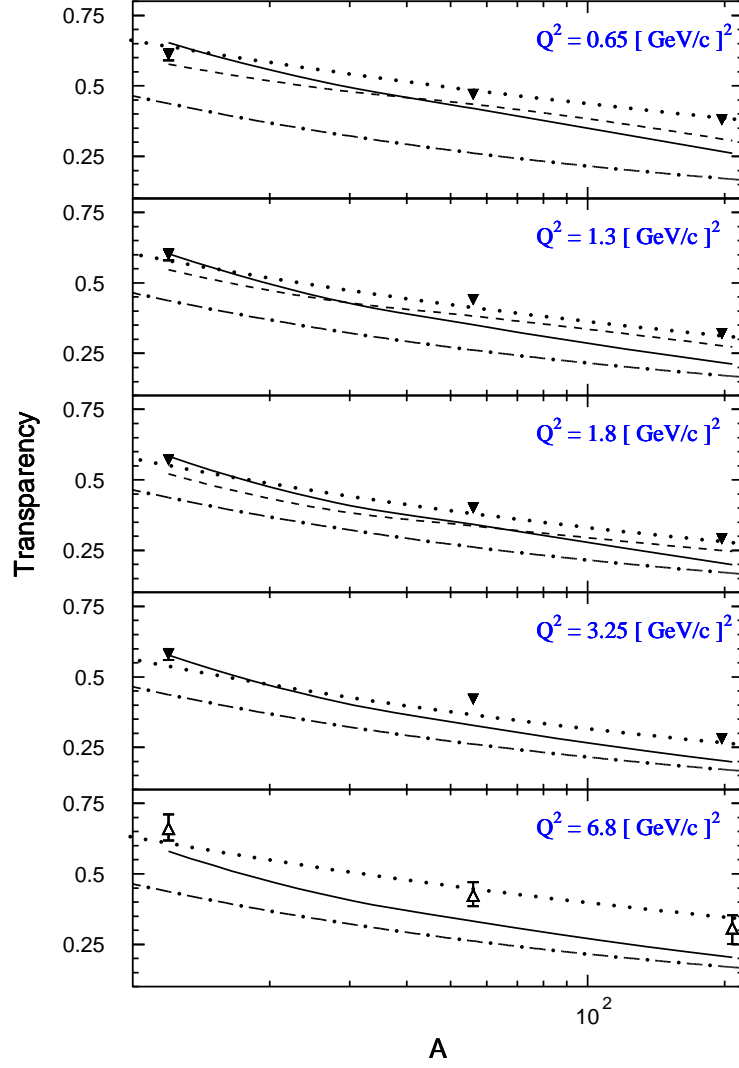


Fig. 4. The A-dependence of the nuclear transparency at five values of the four-momentum transfer Q^2 . The solid (dashed) curves are RMSGGA (RDWIA) calculations. The dotted curves represent the $A^{-\alpha(Q^2)}$ parametrization, while the dot-dashed curve gives $A^{-1/3}$. Data are from [7,8](solid triangles) and [4,5](open triangles).